Scattering times in two-dimensional systems determined by tunneling spectroscopy

J. Smoliner, T. Suski,* C. Gschlössl, W. Demmerle, G. Böhm, and G. Weimann
Walter-Schottky-Institut, Technische Universität München, Am Coulombwall, D-8046 Garching, Germany
(Received 2 June 1992)

On GaAs-$Al_xGa_{1-x}As$ heterostructures, resonant-tunneling processes between two coupled two-dimensional systems are investigated as a function of illumination. With increasing level of illumination, the subband energies and the corresponding spacings between the observed subband resonance peaks are decreased through a reduced depletion field. In addition, large LO-phonon-related satellites of the original subband resonances are observed, which indicate that LO-phonon-assisted processes are the dominant scattering mechanisms in this regime. At high depletion fields, however, electron-plasmon interaction turns out to be the relevant scattering process. Using the amplitude of the phonon satellites as a reference, the field-dependent scattering rate for this process is determined experimentally.

LO-phonon emission has been widely investigated over a long period of time and can be observed in many different types of experiments. In tunneling experiments on single-barrier heterostructures, LO-phonon emission causes extra structures in the tunneling characteristics as soon as the difference between the emitter energy and the collector Fermi level exceeds the LO-phonon energy.[1,2] On double-barrier structures, LO phonons are evident through small satellites of the large negative differential regions, which occur each time an emitter state matches another state inside the well.[3] Moreover, normally forbidden transitions, such as transitions between Landau levels of different indices, become allowed if the momentum conservation parallel to the barriers is violated by phonons.[4,5] To determine the energy-dependent phonon-scattering times in GaAs, ballistic electron transport through vertical and lateral barriers was used.[6,7] Hot-electron luminescence measurements and time-resolved Raman spectroscopy measurements were performed to determine the LO-phonon emission times in bulk GaAs and GaAs-$Al_xGa_{1-x}As$ superlattices, respectively. For bulk GaAs, a phonon emission time of 132 fs was found,[8] whereas in the continuum states of the superlattice the electron-scattering time for LO phonons is about 170 fs.[9] For two coupled asymmetric quantum wells, it was shown experimentally that phonon-assisted tunneling can dominate over impurity-assisted tunneling.[10] In addition, the LO-phonon-assisted intersubband relaxation times were determined for various sample parameters such as different well widths and barrier thicknesses.[11]

In this paper, we investigate the influence of illumination on the tunneling processes between the two-dimensional (2D) subbands of an accumulation layer and an inversion layer. By stepwise illumination, the depletion charge is systematically decreased and the spacing between the tunneling resonances is reduced. In addition, large LO-phonon-related replica peaks of the original subband resonances are observed. The depletion-field dependence of these LO-phonon-related replica peaks is used to determine the scattering rate for electron-plasmon interaction, which becomes the dominant scattering process at higher depletion fields.

The samples consist of an unintentionally p-doped GaAs layer grown on a semi-insulating substrate ($N_A < 1\times10^{14}$ cm^{-3}), followed by an undoped spacer ($d = 50$ Å), doped $Al_xGa_{1-x}As$ ($d = 50$ Å, $n = 4\times10^{18}$ cm^{-3}, $x = 35\%$), another spacer ($d = 100$ Å) and n-doped GaAs ($d = 800$ Å, $n = 1.2\times10^{15}$ cm^{-3}). An additional GaAs cap layer was highly n doped ($d = 150$ Å, $n = 6.2\times10^{18}$ cm^{-3}). Shubnikov–de Haas measurements were used to determine the electron concentrations in the inversion and accumulation layers at liquid-helium temperature ($n^{inv} = 6.3\times10^{11}$ cm^{-2}, $n^{acc} = 5.7\times10^{11}$ cm^{-2}). Ohmic contacts to both channels were aligned using a AuGe alloy. To establish the tunneling contact, a semitransparent AuGe film ($d = 100$ Å) was slightly diffused into the upper GaAs layers. Finally, the GaAs around the top contact was removed selectively, yielding independent contacts to both 2D channels. The resulting band structure is shown in Fig. 1. By applying a bias voltage V_b, the 2D states on both sides of the barrier are shifted energetically with respect to each other. All transitions between these states are directly reflected in the

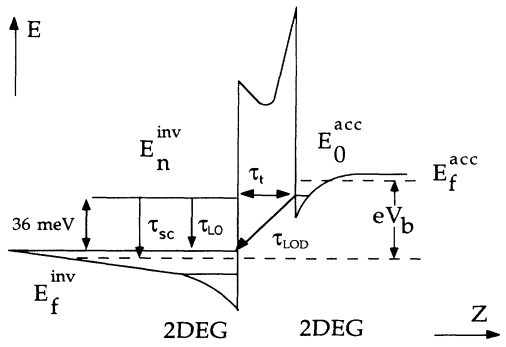

FIG. 1. Schematic band structure of the samples used. τ_t is the tunneling time, τ_{LO} the LO-phonon intersubband scattering time, τ_{LOD} the scattering time for a direct LO-phonon-assisted transition, and τ_{sc} the total scattering time for all other possible relaxation mechanisms.

tunneling current, which allows the determination of the 2D-quantization energies, the observation of Landau-level–Landau-level tunneling and also the determination of tunneling distances in transverse magnetic fields.[12]

To make sure that only one subband is occupied in both 2D systems under any level of illumination, the initial 2D electron concentration was first reduced by hydrostatic pressure. For this purpose, a UNIPRESS clamp cell with light petroleum as a pressure-transmitting medium has been employed. A calibrated highly Te-doped InSb pressure gauge was used to monitor the pressure at temperatures between $T=300$ and 4.2 K. For a typical pressure of $p=3.5$ kbar at low temperature, a reduction of the electron concentration in the lower channel from $n^{\mathrm{inv}}=6.3\times10^{11}$ cm^{-2} to $n^{\mathrm{inv}}=3.9\times10^{11}$ cm^{-2} was achieved. Then the pressurized samples were stepwise illuminated. After each illumination process, the electron density was determined by SdH measurements and the tunneling characteristic was recorded using a four-terminal conductance bridge[13] at a modulation frequency of 22 Hz and a modulation voltage of 0.1 mV.

Figure 2 shows typical IV and dI/dV_b curves traced at $T=4.2$ K and $p=3$ kbar without illumination [curves (1) and (2)] and after illumination [curves (3) and (4)]. In the considered voltage range, the IV curve (1) shows five clear negative differential resistance regions. The single peak at positive bias is due to resonant-tunneling processes from the lowest subband in the inversion layer E_0^{inv} into the lowest subband of the accumulation layer E_0^{acc}. The resonance peaks at negative bias voltages are due to resonance-tunneling processes from E_0^{acc} into the higher subbands of the inversion layer E_n^{inv}. At more negative bias voltages ($V_b<-60$ mV), the resonances smear out to more steplike structures. However, they are still resolved as sharp peaks in the dI/dV_b characteristics [curve (2)]. Typically, 12 resonances can be observed in the range between $V_b=+10$ mV and $V_b=-100$ mV. This reflects the high quality of the sample, since for the highest observed subband the extension of the wave function in the buffer layer reaches values in the order of 2000 Å.

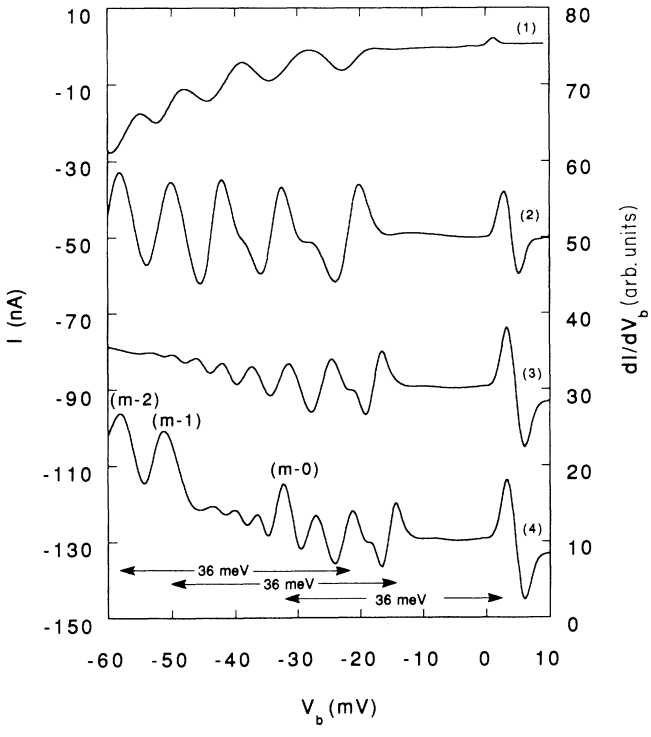

FIG. 2. Typical IV (1) and dI/dV_b (2) characteristics traced at $p=3$ kbar without illumination. With increasing level of illumination, the subband spacing is systematically decreased (3) and LO-phonon-related satellite peaks of the original subband resonances are observed in (4).

Curve (3) shows typical dI/dV_b data after the sample was exposed to four short pulses from a red light-emitting diode (LED). Through the illumination process, the electron density in the lower channel was increased from 4.8×10^{11} cm^{-2} ($p=3$ kbar) to 5.4×10^{11} cm^{-2}. The spacing between the subband resonances is systematically decreased with an increasing level of illumination. In addition, the resonances become weaker and fade out beyond $V_b=-50$ mV. As demonstrated earlier,[12] the 2D subband energies depend mainly on the depletion field in the inversion channel and can be obtained from the measured resonance positions. From the experimental data, we obtain spacings of 20, 7.8, 7.0, and 5.8 mV between the lowest four subband resonance peaks. As demonstrated by self-consistent calculations[14] and magnetotunneling experiments,[15] the subband energy differences on these samples are approximately equal to $\Delta E=e\Delta V_b$, which yields subband energy spacings of 20, 7.8, 7.0, and 5.8 meV, respectively. The depletion field was determined to be 5.1 kV/cm in this case.

If the sample is illuminated further, the subband spacing is further decreased and large LO-phonon-related satellite peaks of the original resonances are observed which have approximately the same size as the subband resonances on the nonilluminated sample. These peaks are denoted as $(m-0)$, $(m-1)$, and $(m-2)$ peaks in curve (4). The $(m-1)$ and $(m-2)$ peaks are observed in a regime where the subband resonances have almost vanished, which makes it difficult to decide whether the satellites are enhanced subband resonances or of different origin. The $(m-0)$ peak, however, clearly coincides with a regular subband resonance. This shows that the observed effect is coupled to the resonant-tunneling process and rules out an involvement of direct LO-phonon-assisted transitions from E_0^{acc} into the subbands of the inversion layer (see Fig. 1). These direct LO-phonon-assisted transitions are only evident as an increase of the background current, as soon as the Fermi energy difference between the two systems exceeds 36 meV ($V_b<-36$ mV). This behavior is explained by the fact that the tunneling rate for this direct transition, $1/\tau_{\mathrm{LOD}}$, is very small compared to the resonant-tunneling rate and therefore no extra peaks are generated.

It must be emphasized that these phonon satellites are also observed at zero pressure. Due to the high electron density at $p=0$ kbar, however, several subbands on both sides of the barrier are occupied after illumination. Thus, many extrastructures in dI/dV_b are generated, making it

difficult to identify single transitions.

Figure 3 shows the amplitudes of the $(m-0)$, $(m-1)$, and $(m-2)$ satellite peaks as a function of the depletion field F, which was obtained from the measured subband energy differences.[12] At high depletion fields, no satellites are observed, and therefore the amplitude is zero above $F=4.5$ kV/cm. Within the experimental error, the amplitudes of all peaks show a broad maximum around $F=3$ kV/cm. At lower depletion fields, which means with an increasing level of illumination, the amplitude decreases again until all satellites vanish below $F=1.5$ kV/cm.

We first consider some basic properties of the charge transfer between the two coupled 2D systems. Two processes are important, which happen in sequence. First, the electrons tunnel resonantly from the emitter electrode into the states of the inversion channel. Second, the electrons relax into the lowest subband and finally to the Fermi level of the collector electrode. Due to the continuity equation, the tunneling current is equal to the "relaxation current," which can be written as

$$I = eNT/\tau_{\mathrm{rel}} , \tag{1}$$

where $1/\tau_{\mathrm{rel}}$ is the relaxation rate averaged over all possible inelastic scattering processes, N is the number of incident electrons, and T the transmission coefficient.

The occurrence of satellite peaks having a distance of 36 mV to the original subband resonances suggests that τ_{rel} is strongly influenced by LO-phonon-induced relaxation processes. As $E_f^{\mathrm{acc}} < \hbar\omega_{\mathrm{LO}}$, intrasubband scattering can be neglected in the target states. It can only occur after the electron is scattered elastically into a lower subband, which is a second-order process. Thus only intersubband scattering processes are now considered in detail. According to the theory developed by Ferreira and Bastard[16] and Weil and Vinter,[17] we have calculated the LO-phonon-assisted intersubband transition rate $1/\tau_{\mathrm{LO}}$ between the mth initial subband and the nth final subband in the inversion channel ($T=0$ K). As a typical example, Fig. 4 shows the results from the $(m-0)$ transition, where we have plotted $1/\tau_{\mathrm{LO}}$ as a function of the corresponding energy differences ΔE_{m-0}. As long as two

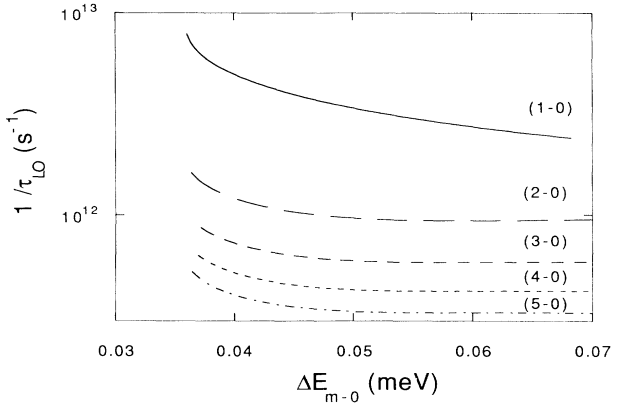

FIG. 4. LO-phonon intersubband scattering times vs subband energy difference ΔE_{m-0} calculated for the $(m-0)$ transitions ($m=1,\ldots,5$).

subbands are separated by less than $\Delta E=36$ meV, LO-phonon-assisted intersubband scattering between these two subbands is not possible. At $\Delta E_{m-0}=\hbar\omega_{\mathrm{LO}}=36$ meV there is a maximum in the intersubband scattering rate, which decreases if ΔE_{m-0} is further increased until it saturates for higher energies. Thus the LO-phonon-assisted intersubband scattering rate shows resonances each time two subbands are separated by $\hbar\omega_{\mathrm{LO}}$. Note that the difference between the maximum of the scattering rate and its saturation value decreases with the increasing subband index of the initial state, which might be the reason that we only observe satellites of the lowest three subband resonances.

Figure 5 shows the calculated LO-phonon-assisted intersubband scattering times τ_{LO}^r for resonant transitions from the mth initial subband into the nth ($n=0,1,2$) final subband ($\Delta E_{m-n}=\hbar\omega_{\mathrm{LO}}=36$ meV) as a function of the depletion field F. In the considered field regime, τ_{LO}^r is in the order of 1 ps for all transitions. From the solid lines, which are an exponential fit to the calculated scattering times, one can see that the scattering times show a roughly exponential behavior on the depletion

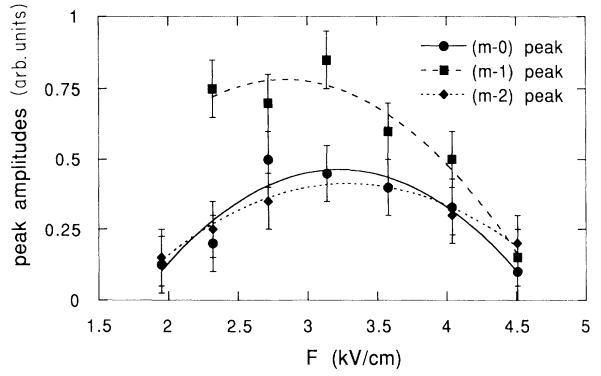

FIG. 3. $(m-0)$, $(m-1)$, and $(m-2)$ LO-phonon satellite peak amplitudes as a function of the depletion field F. The solid lines are guides to the eye.

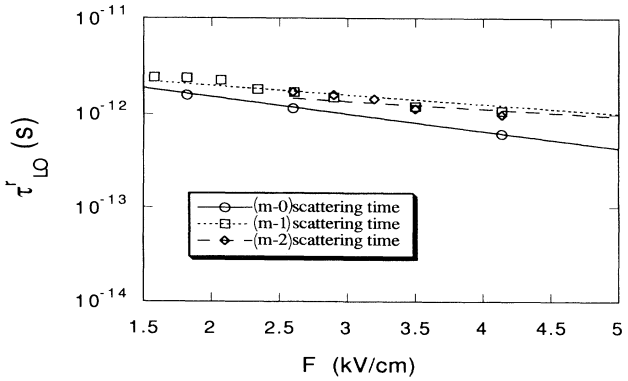

FIG. 5. Resonant LO-phonon scattering times calculated as a function of the depletion field F. The solid lines are an exponential fit to the calculated scattering times.

field F. The scattering time for $(m-0)$ transitions decays faster with increasing depletion field, because the wave function of the lowest subband is always confined at the interface, independent of the depletion field. Thus the wave-function overlap between the mth and the lowest subband strongly depends on F. In contrast to that, the wave function of the first and second exited subband is drastically extended with decreasing depletion field, and therefore the wave-function overlap between the mth and the first subband shows a weaker dependence on the depletion field.

We are now going to demonstrate how the measured phonon peak amplitudes can be used to determine the total scattering times for non-LO-phonon-related scattering processes. Since in Eq. (1) the number of electrons N is proportional to V_b, dI/dV_b will be proportional to the relaxation rate in the lowest-order approximation. This means that $dI/dV_b = A_0 \times 1/\tau_{\rm rel}$, and A_0 is a constant. As mentioned above, $\tau_{\rm rel}$ is obtained by averaging over all possible inelastic-scattering processes. For simplicity, we only distinguish between three different contributions: $\tau^r_{\rm LO}$ is the resonant LO-phonon-assisted intersubband scattering time calculated for situations where two subbands are exactly spaced by $\Delta E = \hbar\omega_{\rm LO}$. This criterion is always fulfilled automatically since the energy differences between the higher 2D subbands become rapidly smaller than 1 meV in our sample. Electrons can also be scattered into a lower subband by nonresonant LO-phonon-assisted transitions with a scattering time of $\tau^{\rm nr}_{\rm LO}$ (see Fig. 6). Finally, $\tau_{\rm sc}$ denotes the scattering time for all other inelastic scattering processes. As all these processes can happen simultaneously, the total scattering time for these processes is calculated as $1/\tau_{\rm rel} = (1/\tau^r_{\rm LO} + 1/\tau^{\rm nr}_{\rm LO} + 1/\tau_{\rm sc})$. Assuming that the electrons return sufficiently quickly to the Fermi energy after phonon scattering, the amplitude A of the phonon satellite peaks in dI/dV_b is then obtained from the difference of the scattering rates calculated with and without resonant LO-phonon intersubband scattering processes.

$$A = A_0[(1/\tau^r_{\rm LO} + 1/\tau^{\rm nr}_{\rm LO} + 1/\tau_{\rm sc}) - (1/\tau^{\rm nr}_{\rm LO} + 1/\tau_{\rm sc})] \ . \quad (2)$$

From Fig. 5, it is obvious that the resonant LO-phonon scattering times $\tau^r_{\rm LO}$ increase with the decreasing depletion field, which is consistent with the decreasing phonon peak amplitudes for values of $F < 3$ kV/cm. In contrast to that, a decreasing satellite peak amplitude with increasing depletion field is observed for $F > 3$ kV/cm. Using Eq. (2), this behavior is only understood if one assumes that $\tau_{\rm sc}$ is much smaller than $\tau^r_{\rm LO}$ at high depletion fields, but much larger than $\tau^r_{\rm LO}$ at low depletion fields. Further, the maximum of the peak amplitudes at $F = 3$ kV/cm and the decreasing peak amplitudes at low depletion fields require that $\tau_{\rm sc}$ is already negligible at the position of the maximum. This offers the possibility to determine the constant A_0 from the maximum of the satellite peak amplitudes if one assumes that $\tau_{\rm sc} = \infty$ at this position. It would be more accurate to use the acoustic-phonon scattering time instead, but Eq. (2) is insensitive to this parameter so that our approximation is justified. Note that the amplitude of the $(m-0)$ peaks is smaller than for the $(m-1)$ peaks, although the scattering rate for the $(m-0)$ transition is larger than for the $(m-1)$ transition. This behavior, however, is understood through the occupied final states for the $(m-0)$ satellites. For this transition only electrons in the energy range between $E_f^{\rm acc}$ and $E_f^{\rm inv}$ can participate in the scattering process. Thus the corresponding satellite peaks are expected to be weak.

The results of the above considerations are plotted in Fig. 7. In the considered range of depletion fields, $\tau_{\rm sc}$ varies between 10 and 0.1 ps for all transitions and the fit (solid lines) yields that $\tau_{\rm sc}$ decays approximately exponentially with increasing F. It is obvious that $\tau_{\rm sc}$ is now allowed to decrease to infinitely small values if the depletion field is further increased. However, a saturation behavior is not observed in the present experiment, since not enough data points could be recorded in this regime. Note that we determine $\tau_{\rm sc}$ for different electron energies when the different phonon satellites $(m-0)$, $(m-1)$, and $(m-2)$ are used. Due to the experimental inaccuracy, however, this energy dependence cannot be resolved.

As shown above, LO phonons are not the dominant scatterers at high depletion fields. Acoustic phonons are known to be extremely inefficient, and therefore the only possible candidate which also acts as an effective inelastic scattering process is electron–2D-plasmon scattering.[18–20] Plasmons were also directly detected in tunnel-

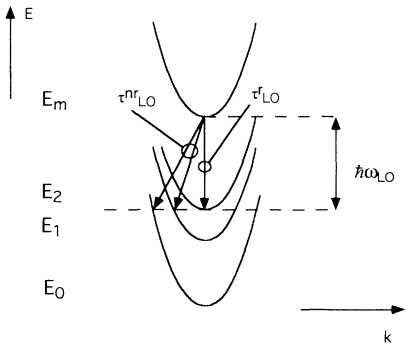

FIG. 6. Schematic view of resonant and nonresonant LO-phonon-assisted intersubband scattering processes.

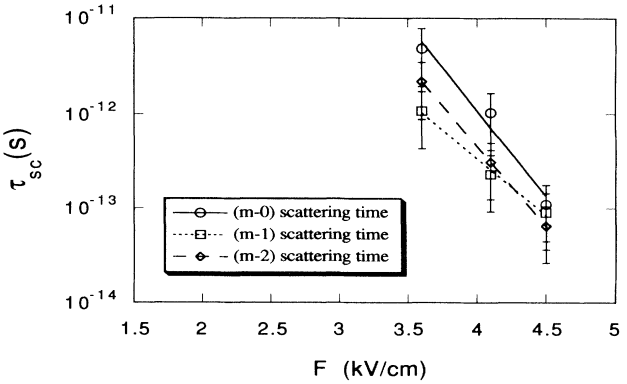

FIG. 7. Measured scattering times for electron-2D-plasmon processes. The solid lines are obtained by fitting an exponentially decaying curve to the experimental data.

ing experiments; depending on the device structure, however, they were found to be of differing importance.[21,22] Using a simple one-band model, Giuliani and Quinn[23] have calculated the lifetimes of 2D electrons which are scattered by 2D plasmons. Higher subbands as well the shape of the potential were not taken into account, and therefore a field dependence of the scattering times cannot be obtained from this model. However, it can be used to obtain the order of magnitude of τ_{sc} for electron-plasmon scattering processes. Using typical parameters for a nonilluminated sample, we find scattering times on the order of 5×10^{-14} s for our situation. This means, that electron-2D-plasmon scattering is one order of magnitude faster than LO-phonon scattering at high depletion fields, which is consistent with the results obtained experimentally for τ_{sc}. Also, the strong dependence of τ_{sc} on the depletion field is understood in terms of this model. Similar to the LO-phonon scattering rate, the plasmon scattering rate depends on the matrix element between the initial and final states. In the matrix element, the phonon scattering potential is equal to $\exp(-Q|z-z'|)$,[23] the plasmon scattering potential, however, is a Coulomb potential which is equal to $e/(4\pi\epsilon_0|z-z'|)$ if no screening is assumed for simplicity. Thus the plasmon scattering rate diverges at high depletion fields, which means when the wave functions of the initial and final states are close in real space. Note that this is also consistent with the assumption that electrons relax sufficiently fast to the Fermi level after a resonant LO-phonon scattering process. After phonon scattering into a lower subband, the electrons are more closely confined to the interface and, therefore, the plasmon-related relaxation rate to the Fermi energy will be high.

In summary, tunneling spectroscopy was used to investigate the dominant relaxation processes for 2D electrons in a variable potential. At low depletion fields in the 2D channel, resonant LO-phonon-assisted intersubband scattering was found to be the dominant process, which was verified through large LO-phonon-related satellite peaks in the tunneling characteristics. For high depletion fields, however, a different scattering process becomes dominant, whose depletion-field-dependent scattering time was determined using the amplitudes of the LO-phonon resonance peaks as a reference. As both the magnitude and the depletion-field dependence of the measured scattering times is consistently explained, we find justification for our interpretation of electron-2D-plasmon interaction being the relevant scattering process at high depletion fields.

The authors are grateful to Peter Vogl and Daniel Oberli for helpful discussions. Technical assistance was provided by Michael Fischer and Rudolf Koch. This work was sponsored by BMFT Project No. TK 0368/7.

*Permanent address: Unipress, High Pressure Research Center, Polish Academy of Science, ul. Sokolowska 29/37, 01-142 Warszawa, Poland.

[1]T. W. Hickmott, P. M. Solomon, F. F. Fang, F. Stern, R. Fischer, and H. Morkoc, Phys. Rev. Lett. **52**, 2053 (1984).
[2]Pong-Fei Lu, D. C. Tsui, and H. M. Cox, Appl. Phys. Lett. **45**, 772 (1984).
[3]V. J. Goldmann, D. C. Tsui, and J. E. Cunningham, Phys. Rev. B **36**, 7635 (1987).
[4]R. E. Pritchard, P. C. Harness, L. Cury, J. C. Portal, B. Khamsehpour, W. S. Truscott, and K. E. Singer, Semicond. Sci. Technol. **6**, 626 (1991).
[5]M. L. Leadbeater, E. S. Alves, L. Eaves, M. Henini, O. H. Huges, A. C. Celeste, and J. C. Portal (unpublished).
[6]M. Heiblum, D. Galbi, and M. Weckwerth, Phys. Rev. Lett. **62**, 1057 (1989).
[7]U. Sivan, M. Heiblum, and C. P. Umbach, Phys. Rev. Lett. **63**, 992 (1989).
[8]W. Hackenberg and G. Fasol, Appl. Phys. Lett. **57**, 174 (1990).
[9]K. T. Tsen and H. Morkoc, Phys. Rev. B **38**, 5615 (1988).
[10]D. Y. Oberli, J. Shah, T. C. Damen, J. M. Kuo, J. E. Henry, J. Lary, and S. M. Goodnick, Appl. Phys. Lett. **56**, 1239 (1990).
[11]B. Deveaud, A. Chomette, F. Clerot, P. Auvray, R. Regreny, R. Ferreira, and G. Bastard, Phys. Rev. B **42**, 7021 (1990).
[12]W. Demmerle, J. Smoliner, E. Gornik, G. Böhm, and G. Weimann, Phys. Rev. B **44**, 3090 (1991).
[13]R. Christanell and J. Smoliner, Rev. Sci. Instrum. **59**, 1290 (1988).
[14]J. Smoliner, G. Berthold, G. Strasser, E. Gornik, G. Weimann, and W. Schlapp, Semicond. Sci. Technol. **5**, 308 (1990).
[15]J. Smoliner, E. Gornik, and G. Weimann, Phys. Rev. B **39**, 12 937 (1989).
[16]R. Ferreira and G. Bastard, Phys. Rev. B **40**, 1047 (1989).
[17]T. Weil and B. Vinter, J. Appl. Phys. **60**, 3227 (1986).
[18]M. V. Fischetti, Phys. Rev. B **44**, 5527 (1991).
[19]K. Diff and K. F. Brennan, J. Appl. Phys. **69**, 3097 (1991).
[20]N. S. Mansour, K. Diff, and K. F. Brennan, J. Appl. Phys. **69**, 6506 (1991).
[21]C. B. Duke and M. J. Rice, Phys. Rev. **181**, 733 (1969).
[22]K. Kim and K. Hess, J. Appl. Phys. **64**, 3057 (1988).
[23]G. F. Giuliani and J. J. Quinn, Phys. Rev. B **26**, 4421 (1982).